

Numerical Analysis of an Ultrasonic Technology for Food Dehydration Process Intensification

Roque R. Andrés¹, Olivier Louisnard², Enrique Riera¹, Victor M. Acosta¹

¹Grupo de Sistemas y Tecnologías Ultrasonicas (GSTU), ITEFI, CSIC; Madrid, España

²Centre RAPSODEE UMR CNRS 5302. École des Mines d'Albi, Albi, Francia

*roque.andres@csic.es

Abstract: Industrial processes assisted by high-power ultrasound have become an attractive field for industries because of its sustainability (low energy consumption, non-pollutant processes) and efficiency. Among these processes we can find food dehydration aided by ultrasound, based on the proper exploitation of the non-linear effects associated to finite-amplitude-wave propagation that are able to enhance mass transfer processes in this case.

In this work, the design of a new high-power ultrasonic transducer for food dehydration intensification and the effects produced on food samples located inside a dehydration chamber have been performed using COMSOL Multiphysics®.

Keywords: power ultrasound, mass transfer processes, food dehydration, power ultrasonic transducers, ultrasonic propagation.

1. Introduction

Industrial processes assisted by high-power ultrasound (HPU) have become a new, green and efficient technology with a great potential in its implementation. Previous researches like [1, 2] show that these HPU technologies provide a good performance in processes like particle agglomeration or defoaming, among others. In the particular case of food dehydration at low temperature (atmospheric freeze drying), it has been proved by [3] that HPU provides a faster and more economic performance, improving also the quality of the final product.

In order to provoke the desired effects on the samples, it is necessary to generate a stable high level ultrasonic field, covering a wide volume in gas media. Previous researches indicated that the right devices to produce this ultrasonic field are the high-power ultrasonic transducers with extensive radiators [4].

Anyway, the development of this kind of devices has to deal with the need of a high level ultrasonic field in a gas media, with a good

impedance matching between the radiator and the gas and a high amplitude of vibration in the radiating plate [5].

The first stage in the developing process of a high-power ultrasonic transducer with extensive radiator is the design of the device applying numerical methods [6], obtaining the eigenfrequencies of the system and determining the efficiency when radiating on a fluid media.

The main objective of this work is to present the mechanical and acoustical analysis done using COMSOL Multiphysics® over a new high power ultrasonic transducer with a stepped-grooved circular plate radiator for food dehydration process intensification, as well as the parametric study of the sample location inside the chamber, in order to optimize the system efficiency.

2. Use of COMSOL Multiphysics

The mathematical model, including the Structural Mechanics Module, the Acoustic Module and the Multiphysics analysis of COMSOL Multiphysics 5.0® allowed us to determine the influence of the different constitutive parts of the transducer, as well as the generated ultrasonic field inside a dehydration chamber where the samples were placed.

The transducer is composed by two groups of two piezoelectric ceramic stacks separated by a brass flange, two attached steel masses and a mechanical amplifier (or horn). The stepped-grooved circular plate transducer is bolted at the horn's tip. The whole system's mechanical behavior has been studied, considering the masses, the horn and the circular radiator as linear elastic materials with isotropic behaviour.

The whole study has been taken considering a 2D axisymmetric component for the whole transducer but including partial 3D studies to identify other vibration modes of the circular radiator and of the brass flange. This study includes the modal analysis of the transducer and the acoustic field in the drying chamber.

2.1 Grooved-stepped circular plate

The stepped-grooved circular radiator is excited in its center by the vibrator with a displacement at the desired operational mode. This plate generates a coherent ultrasonic field in the acoustic chamber due to the stepped profile of the front face [7], and a focused ultrasonic field in the other side due to the grooves applied in the back face [5].

A 3D model has been done for the circular titanium radiator in order to identify the desired vibration mode with seven nodal circles (7NC) and other close modes that may have adverse effects when working at its operational mode [8]. The physic considered in this case has been a Solid Mechanics, defining the plate as a Linear Elastic Material and applying the following equation (1) to obtain the eigenfrequencies of the plate:

$$-\rho\omega^2\mathbf{u} = \nabla\sigma \quad (1)$$

where ρ denotes the density, ω the angular frequency, \mathbf{u} is the displacement vector and \mathbf{F}_v the force vector.

Figure 2 shows the 7NC shape at 24884Hz, obtained applying a swept mesh shown figure 1. Other close modes can be observed in figure 3:



Figure 1. Swept mesh for the circular plate.

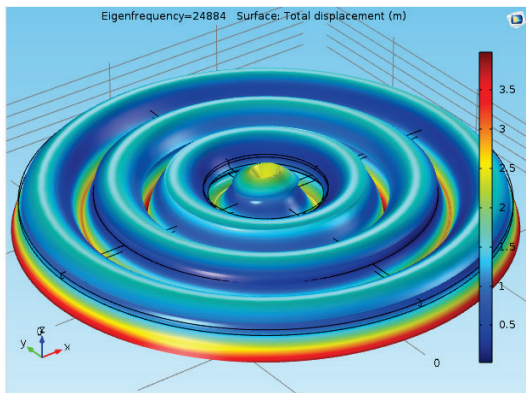


Figure 2. Mode shape with 7NC at 24884 Hz.

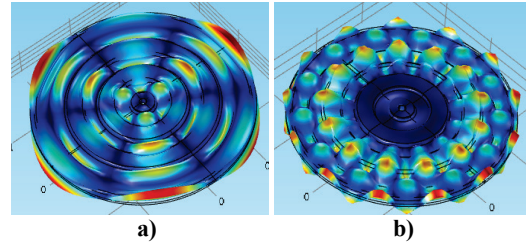


Figure 3. a) Mode shape with 7NC, 3 diameters and a flexural mode at 25929 Hz. b) Mode shape with a combination of different shapes (NC, diameters...)

2.2 Vibrator

The vibrator is composed by the Langevin-type transducer (or sandwich) and the horn.

On one side, the sandwich is made up by four piezoelectric ceramics, the brass flange, the front mass and the back mass. The thickness of the masses (l_i) depends on the required operational frequency (ω) and on the properties of the ceramics (l_c , sound speed c_c , density ρ_c and area A_c) and of the material used for the masses (c_i , ρ_i y A_i), and applying the equation (2), shown in [9]:

$$\tan\left(\frac{\omega l_c}{c_c}\right)\tan\left(\frac{\omega l_i}{c_i}\right) = \frac{\rho_c c_c A_c}{\rho_i c_i A_i} \quad (2)$$

The electro-mechanical transduction takes place in the piezoelectric ceramics, applying the piezoelectric constitutive equations (3,4) for the stress-charge form:

$$T = c_E S + e^T E \quad (3)$$

$$D = eS + \epsilon_0 \epsilon_r E \quad (4)$$

Where T is the mechanic stress, S is the strain, E is the electric field and D is the electric displacement. On the other side, c_E corresponds to the elasticity matrix, e is the coupling matrix and ϵ is the permittivity.

In this work, the corresponding material for the piezoelectric ceramics is a PZT-802 compound and the masses are made of structural steel.

On the other side, the aim of the titanium horn is to amplify the extensional displacement in the front mass and consists on a $\lambda/2$ rod with two circular sections (S1 and S2), each with a $\lambda/4$ length.

In this case, a Piezoelectric Device has been considered, in which the ceramics are defined as a Piezoelectric Material.

Figure 4 shows the initial model for the vibrator and figure 5 shows the amplification rate obtained for the extensional mode of 27036 Hz:

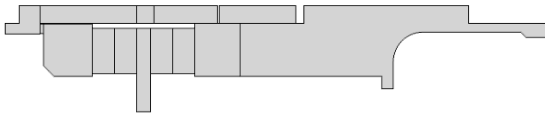


Figure 4. Model of the vibrator

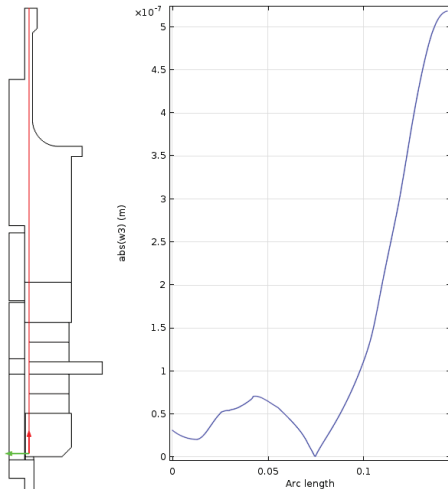


Figure 5. Amplification rate in the horn

2.3 Complete transducer

The next step consists on joining the vibrator and the plate, and simulating the whole system considered as a Piezoelectric Device that includes Solid Mechanics and Electrostatic Physics, and applying an extra fine mesh, as shown in figure 6:

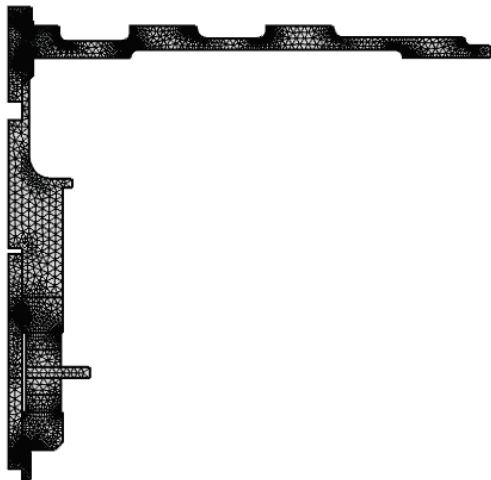


Figure 6. Extra fine mesh applied for the transducer simulation.

The analysis of the modal behaviour of the transducer has to be done in three steps. A first stationary study to simulate the 25 MPa prestress to be applied in the ceramics [6]. In order to simulate this prestress in a 2D axisymmetric model is necessary to apply a boundary load in the bolt and a fixed constraint in the base of the transducer. In figure 7, the stress obtained in the ceramic stack in the Stationary study is shown:

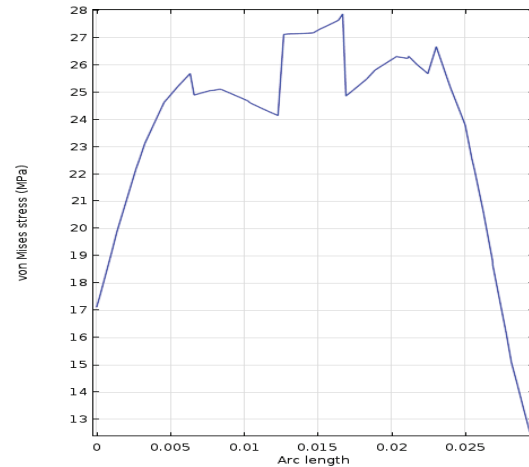


Figure 7. Prestress in the ceramic stack.

Once the prestress has been determined, the next stage is to obtain the eigenfrequencies and the mode shapes, applying the equation (1). In this case, a 7NC mode has been obtained at 25427 Hz.

The third task is to do a Frequency Domain study, applying an excitation voltage of 100 V, at a frequency around the desired mode obtained. In this case, a parametric study has been done, for different frequencies, in order to identify the most efficient operating frequency around the 7NC mode.

After the simulation, the most efficient working frequency has been found at 25445 Hz, as shown in the figure 8, with the admittance of the ceramics.

The mode shape at 25445 Hz, with a maximum amplification rate in the horn and a 7NC mode in the circular radiator is shown in figure 9.

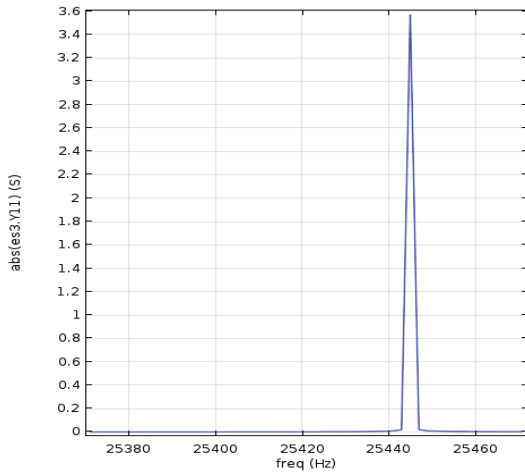


Figure 8. Admittance in the ceramics for different excitation frequencies.

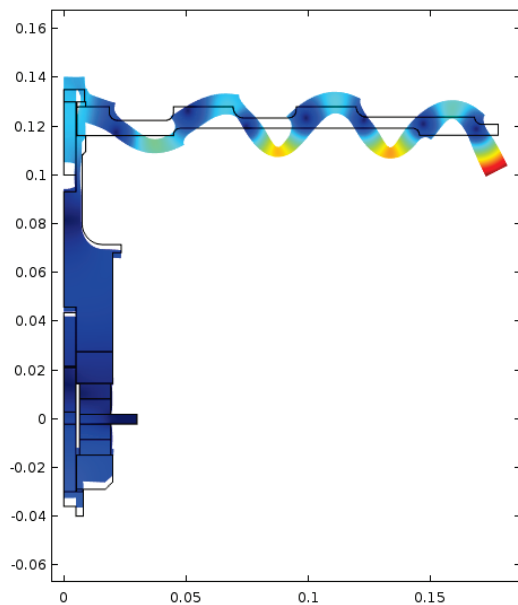


Figure 9. Vibration shape at the working frequency.

2.4 Ultrasonic field

As it has been mentioned before, the application of steps in the circular plate's surface provides a coherent acoustic radiation in the fluid media, generating a plane wave like a circular piston [5]. The acoustic field generated by a circular piston has been widely studied by [10, 11] and the equations to determine the acoustic propagation or calculate the amount of radiated, dissipated or absorbed energy are used in the finite element method.

In this case, the acoustic field inside a cylindrical dehydration chamber has been studied, considering an ultrasonic propagation in air at 20°C, with thermal and viscous losses. The governing equation for the ultrasonic field is the wave equation with losses (5):

$$\nabla \cdot \left(-\frac{1}{\rho_c} (\nabla p_t - \mathbf{q}_d) \right) - \frac{k_{eq}^2 p_t}{\rho_c} = Q_m \quad (5)$$

where the losses appear in the effective density (ρ_c) and wave number (k_{eq}).

The dehydration chamber has been defined as a Sound Hard Boundary, taking into account that steel wall may have a similar behaviour as a 100% reflecting wall [8].

The acoustic field simulation involves a Multiphysics analysis, including electrostatic, solid mechanic and pressure acoustic physics.

The main ultrasonic source is the stepped-grooved circular radiator because the highest displacements take place in this area. In any case, the rest of the transducer's surfaces may have a small influence on the near ultrasonic field.

Finally, in order to determine the most efficient mesh in the ultrasonic field, a convergence analysis was performed in [12]. In this case, a free triangular mesh with a maximum size of $\lambda/16$ was selected.

The acoustic field inside the dehydration chamber, for an excitation frequency of 25445 Hz is shown in figure 10, for absolute values of acoustic pressure (Pa), and in figure 11 for the acoustic pressure levels (dB).

The different behaviour of the stepped and the grooved faces can be observed in figure 10. The upper half of the chamber, influenced by the stepped face, shows a more or less coherent field, but with a maximum along the axis due to reflections in the wall. On the other side, the lower half of the dehydration chamber is affected by the grooved side of the radiator, and the energy is focused at a distance around 30-40 cm from the circular plate.

Figure 11 indicates the maximum acoustic levels obtained in the ultrasonic chamber, with values around 160 dB in the axis.

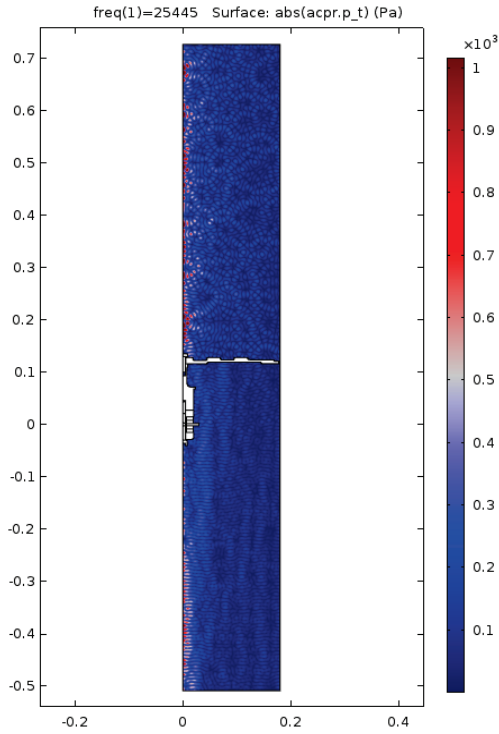


Figure 10. Acoustic pressure (Pa) in the dehydration chamber.

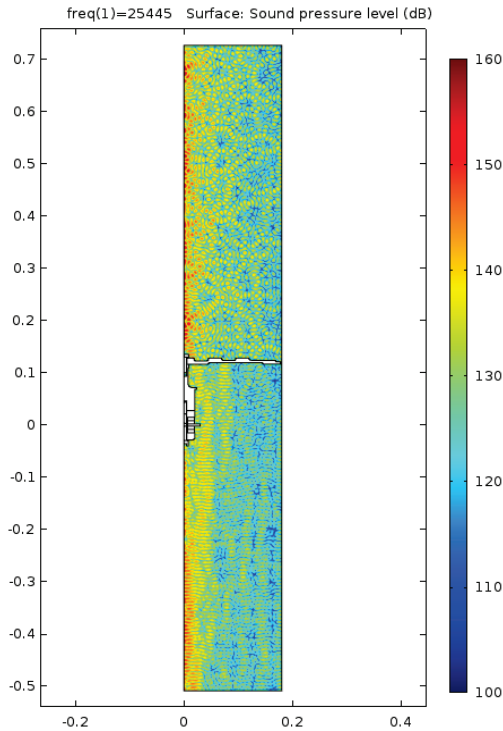


Figure 10. Acoustic pressure level (dB) in the dehydration chamber.

2.5 Simulation of a food sample in the dehydration chamber.

As indicated in [8], the drying kinetics inside a dehydration chamber depends on how does the food sample absorb the acoustic energy inside the chamber.

There are two aspects to take into account. First of all is that the ultrasonic field is not uniform along the whole chamber, therefore, it is important to define the areas where the acoustic energy is higher.

The other aspect to consider is the absorption power of the samples to dry. In [8], the acoustic properties of a potato sample were defined, in order to obtain the effective density (ρ_e) and sound speed (c_e) according to the equations (6,7):

$$\rho_e = \rho_p \left(1 + \frac{i\phi}{\rho_p \omega} \right) \quad (6)$$

$$c_e = c_p \left(1 + \frac{i\phi}{\rho_p \omega} \right)^{-\frac{1}{2}}, \quad c_p = \sqrt{\frac{1}{\rho_p k_p \Omega}} = \frac{c}{\sqrt{\Omega}} \quad (7)$$

According to these equations, the values for the effective density and sound speed are the following:

Table 1: Acoustic properties of a potato sample

Effective density (kg/m ³)	Effective sound speed (m/s)
$1.21 + i 1.15 \cdot 10^8$	$0.176 + i 0.176$

The sample is modelled in COMSOL Multiphysics® as a square domain located inside the fluid, with a 20 mm side. This domain is defined as a linear elastic fluid with the acoustic properties indicated in the Table 1. The imaginary parts of the effective sound speed and density determine the energy losses (related to the dehydration power) in the samples.

In order to determine the optimal area to place the sample inside the chamber, a parametric study has been done. This simulation consists on the determination of the ultrasonic field generated by the transducer inside the dehydration chamber, placing the 20 mm square sample in the chamber and moving it along the whole surface.

In order to determine how the sample dissipates the acoustic energy, and where is the area with a maximum absorption, we can define a volume integration in the sample, applying the equation (8):

$$\iiint_V -\phi|U|^2 dV \quad (8)$$

where ϕ denotes the sample flow resistance and U is the RMS speed. The result is the energy dissipation (in Watts) inside the food sample.

The distribution of the energy absorption determined after the integration of the results obtained after the parametric study is shown in the figure 11:

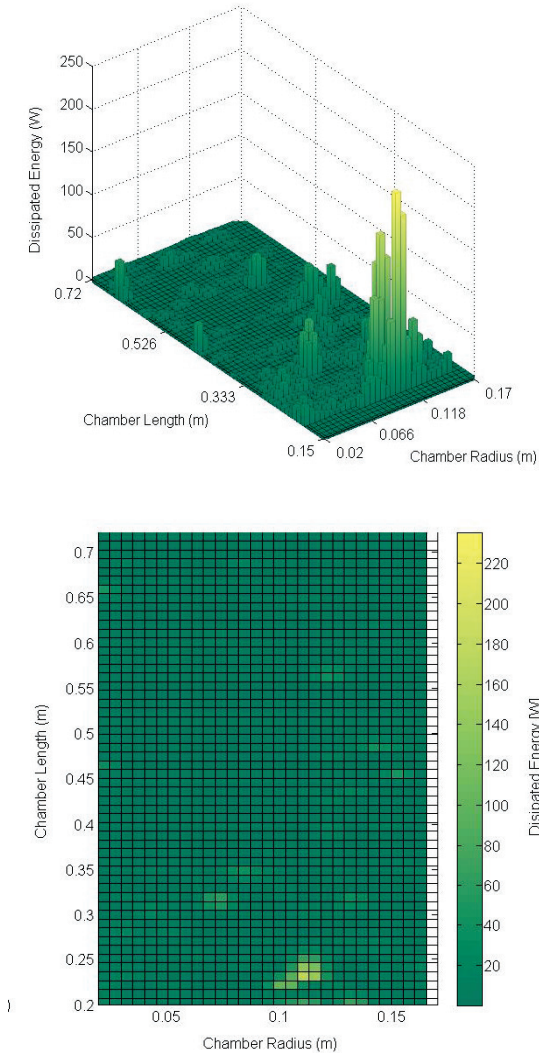


Figure 11. Distribution of the dissipation power of the potato sample along the dehydration chamber.

This last simulation indicates that the area with a highest energy absorption is situated near the radiator at about 10-12 cm from the axis.

3. Conclusions

The complete numerical analysis of an ultrasonic-based dehydration technology has been taken using COMSOL Multiphysics®.

This technology consists on a HPU transducer generating a HPU field inside a dehydration chamber, where the food samples lie.

The study comprised the modal analysis of the constitutive parts and of the whole HPU transducer, the ultrasonic field generated by the transducer working at its operational mode and the energy absorption of a simulated potato sample located inside the dehydration chamber.

The designed system works at the operational frequency of 25445 Hz, generating an ultrasonic field with values around 160 dB in the axis.

The area with the highest energy absorption is situated near the circular radiator and the wall of the chamber.

4. References

1. E. Riera, I. González-Gomez, G. Rodríguez, and J. A. Gallego-Juárez, "Ultrasonic agglomeration and preconditioning of aerosol particles for environmental and other applications," in *Power Ultrasonics*, J. A. Gallego-Juárez and K. F. Graff, Eds., ed Oxford: Woodhead Publishing, pp. 1023-1058 (2015).
2. G. Rodríguez, E. Riera, J. A. Gallego-Juárez, V. M. Acosta, A. Pinto, I. Martínez, *et al.*, "Experimental study of defoaming by air-borne power ultrasonic technology," *Physics Procedia*, vol. 3, pp. 135-139 (2010).
3. J. V. Garcia-Perez, J. A. Carcel, E. Riera, C. Rosselló, and A. Mulet, "Intensification of low-temperature drying by using ultrasound," *Drying Technology*, vol. 30, pp. 1199-1208, (2012).
4. J. A. Gallego-Juarez, G. Rodriguez-Corral, and L. Gaete-Garreton, "An ultrasonic transducer for high power applications in gases," *Ultrasonics*, vol. 16, pp. 267-271 (1978).
5. J. A. Gallego-Juarez, G. Rodriguez, V. M. Acosta-Aparicio, and E. Riera, "Power ultrasonic transducers with extensive radiators for industrial processing," *Ultrasonics Sonochemistry*, vol. 17, pp. 953-64 (2010).
6. E. Riera, J. V. García-Pérez, J. A. Cárcel, V. M. Acosta-Aparicio, and J. A. Gallego-Juárez, "Computational study of ultrasound-assisted drying of food materials," in *Innovative Food Processing Technologies: Advances in*

Multiphysics Simulation, ed: Blackwell Publishing Ltd., pp. 265-301 (2011).

7. A. Barone, "Flexural vibrating free-edge plates with stepped thickness for generating high directional ultrasonic radiation," *The Journal of the Acoustical Society of America*, vol. 51, pp. 953-959 (1972).

8. R. R. Andrés, O. Louisnard, E. Riera, and V. M. Acosta, "Study of the near field generated by a power ultrasonic transducer," in *Euroregio 2016*, Porto (Portugal), (2016).

9. E. Neppiras, "The pre-stressed piezoelectric sandwich transducer," *Ultrasonics international 1973*, pp. 295-302 (1973).

10. L. E. Kinsler and A. P. Frey, *Fundamentals of acoustics*: John Wiley & Sons (1950).

11. P. M. Morse and K. U. Ingard, *Theoretical acoustics*: Princeton university press (1968).

12. R. R. Andrés, "Memoria justificativa estancia Universidad de Toulouse 2015," Informe técnico 2015.

5. Acknowledgements

This work has been supported by the project DPI2012-37466-C03-01 funded by the Spanish Ministry of Economy and Competitiveness.